# ASME Human Powered Vehicle Challenge

# PANTHER 1

# Team #22


**Team Advisor:**

Dr. David Schmidt
Benedum Hall
Pittsburgh, PA 15213
Email: des53@pitt.edu

**Team Members:**

Abe Stucky (President)
Rob Ward
Rob Schrameyer
Erin Sarosi
Michael Sackandy
Kevin Weldon
Zach Yoder
Zach Lynn
Ryan Mitchell
Sean Handerhan
Ethan Linderman
Jeremiah Hoydich
Sinjon Bartel

## 3-View Drawing of Vehicle

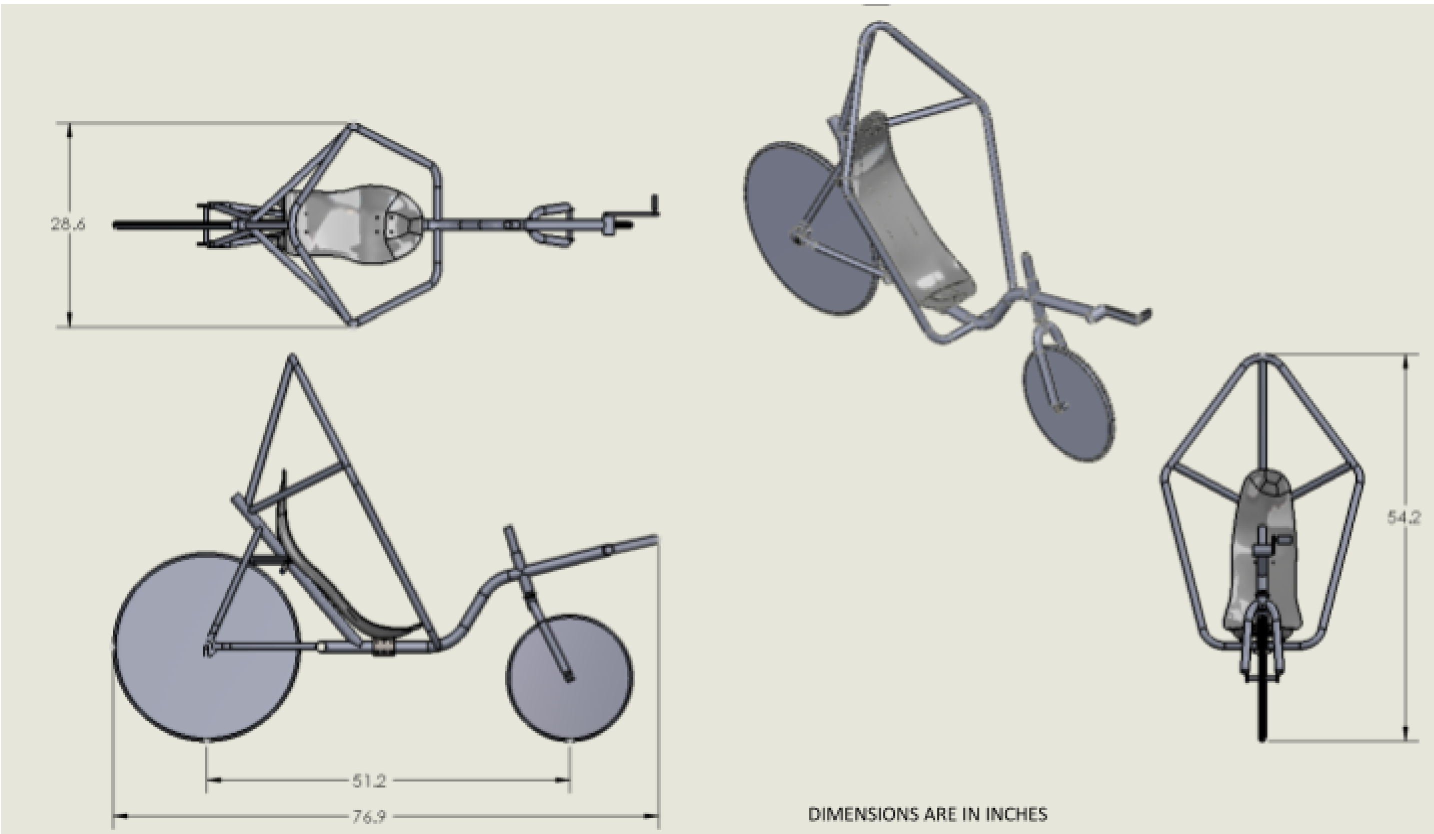

## Abstract

During the 2016-2017 academic year, the Pitt HPVC team designed and constructed our first human powered vehicle for the competition. After performing initial research on types of recumbent vehicles, the team decided to design a low-rider recumbent bicycle style vehicle with the main goals of manufacturability and functionality in mind. Since the team is new, we have relied on outside research, faculty mentorship, and advice from the school's Formula SAE team in order to create a successful vehicle.

The bicycle was designed with a 4130 chromoly steel frame and roll cage and front wheel steering. The frame was designed to be simplistic for ease of welding and fabrication, and the tubing sizes have been optimized for cost, weight and strength. The seat will be adjustable to allow for different sized riders to race the bike comfortably.

## Table of Contents

# 1. Design

## 1.1 Objective

The design goal is to develop structural concepts, analyze, and fabricate a complete bicycle, including a frame and rollover protection system based on the ASME HPVC competition rules. Additional goals for Pitt's club include:

- Develop a logbook and design process that future Pitt teams can use as a guide in future years
- Complete all events in the HPVC East competition
- Make the vehicle compatible for riders 5'4" to 6'0"

## 1.2 Background

### 1.2.1 Frame Geometry

Design started by researching existing geometries of recumbent bicycles and human powered vehicles. Club member Rob Schrameyer attended the competition in 2016 and reported that the fastest bikes were two-wheeled, so early on we mainly considered two-wheeled designs. Later we re-evaluated this decision with a Pugh chart (see Section 1.5.1). The following images are from early research.

*Figure 1: Fast recumbent design where the driver is low to the ground*

[https://albrechtmba.wordpress.com/2013/08/21/recumbent-encounters-of-the-fast-kind/]

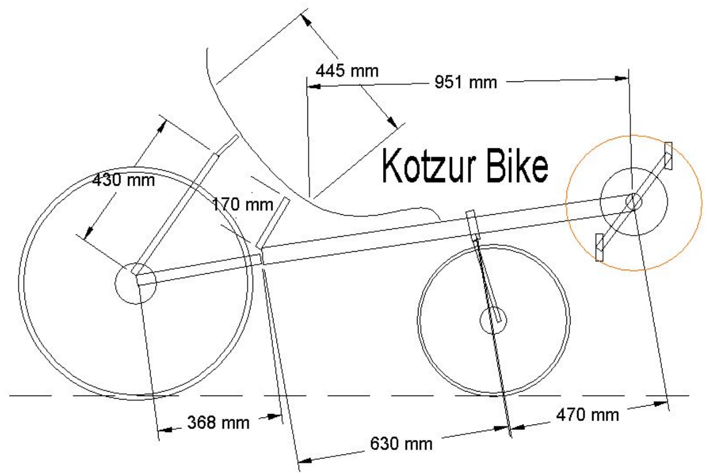


*Figure 2: Kotzur Bike - The rider is higher off of the ground, but manufacturing would be easier with no tube bending required.*
*[https://s-media-cache-ak0.pinimg.com/originals/8c/e2/34/8ce234508f04651fe5576453a6cd3c4e.gif]*


*Figure 3: An innovative tricycle design and description from the University of Colorado. The bicycle features an adjustable bottom bracket/chain tensioner, cargo storage behind the seat, and a partial fairing.*
*[https://sites.google.com/site/dhipwooddigitalportfolio/projects/human-powered-vehicle]*

Early frame geometry decisions were made based off of experience riding regular bicycles. For example, the head tube angle of 72 degrees was based off of club president Abe Stucky's touring bike called the Surly Long Haul Trucker because a reclined angle makes the steering less "twitchy".[1] Other geometry choices were made from bicycle fitting websites; for example, road racing bicycles have a seat tube angle of 73 degrees.[2] The bottom bracket height (680mm) was based on the Optima Lynxx recumbent bike.[3] To determine wheel size, we looked at Sheldon Brown's web page on wheel and tire sizing and selected a 700C (622mm ISO) rear wheel and 20 in (406mm ISO) front wheel.[4] An early sketch of the frame geometry can be seen in Figure 4.

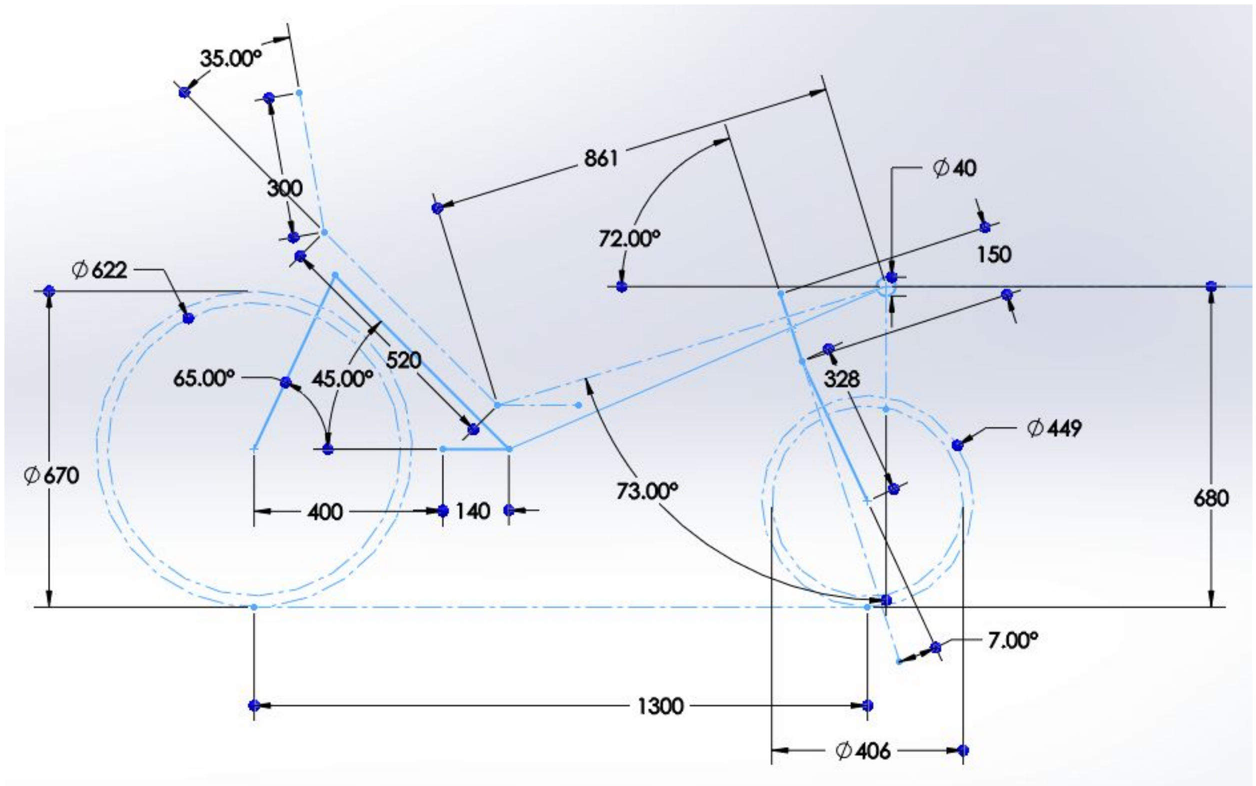


*Figure 4: Frame geometry from October 2016*

## 1.3 Prior Work

Prior to the 2016-2017 school year, no design, fabrication or testing was done on the vehicle. This is the University of Pittsburgh's first year in the HPVC competition and all designs are new to the team.

## 1.4 Design Specifications

We began our design by referencing design specifications provided by the competition. These included:

- Complete a turn within an 8 meter radius
- Stop from a speed of 25 km/hr in a distance of 6.0 meters
- Demonstrate stability for at least 30 meters while traveling at 5-8 km/hr
- Ensure safety for the rider when a 2670 N force is applied to the roll cage at 12° from vertical and prevent more than 5.1 cm deflection
- Ensure safety for the rider when a 1330 N force is applied to the roll cage horizontally and prevent more than 3.8 cm deflection
- Provide space for on either side of the vehicle for 35x30 cm ASME decals and 10x20 cm space for high contrast Pitt decals

Furthermore, we have provided our own specifications for the vehicle to ensure its functionality:

- Incorporate adjustability from riders between 5'4" to 6'0"
- As a rule of thumb, use a factor of safety 3 for calculations[7]

## 1.5 Concept Development and Selection Methods

### 1.5.1 Vehicle Type

The following Pugh chart was used during the concept phase to determine design characteristics. Since this is our first year in the competition, we weighted features such as manufacturability, stability, and handling as most important. Each design team member chose numbers for each category based on intuition, and the numbers were averaged into the table below. From this we made an early decision to go with a two-wheeled design.

*Table 1: Vehicle Type Pugh Chart.*

| **Design Feature** | **Manufactur-ability/Cost** | **Speed** | **Stability** | **Handling /Agility** | **Weight** | **Aerodynamics** | **TOTAL (out of 10)** |
|---|---|---|---|---|---|---|---|
| *Weighted Scale* | *.3* | *.1* | *.2* | *.2* | *.1* | *.1* | *10* |
| Two-Wheel Design | 7.3 | 7.3 | 3.3 | 5 | 7.3 | 6.6 | 5.97 |
| Three-Wheel Design | 5 | 5 | 7.3 | 6.6 | 5.3 | 4.3 | 5.74 |

### 1.5.2 Steering System

The different steering options considered were under seat steering (USS), over seat steering (OSS), and double head tube steering (DHTS).

Under seat steering (Figure 5) is fairly common among two- and three-wheel recumbent bicycles. USS is a simple method of steering to learn and offers a more natural hand placement during the ride. In USS systems, handlebars are located near the seat, ensuring that they are never in the way of the rider, and can be connected directly to the wheels by a tie rod or a series of linkages. USS design handlebars could alternatively act as effective handholds when trying to generate powerful pedal strokes. The primary drawbacks of a USS system are the more complex and heavier design elements, a higher overall cost, additional drag due to a larger frontal area, and the need to weld materials together.

*Figure 5: Under Seat Steering (USS) design.*
*[http://www.hpvelotechnik.com/produkte/ghp/details_e.html]*

The over seat steering (OSS) system (Figure 6) incorporates handlebars above the frame of a recumbent bicycle. OSS implements the counter steering method, commonly used in upright bicycles. The rider need only swing the handlebar back in the opposite direction of desired travel, making this method natural and easy to learn. Recumbent bicycles have handlebars that extend a considerable distance behind the front wheel, similar to tillers on a boat's rudder steering system. OSS systems are the simplest and most adjustable design, very easy to master without prior experience, and more aerodynamic than USS systems. The only considerable drawback of an OSS design is the awkward steering motion and limited range of movement caused by a long handlebar extender.

*Figure 6: Over seat steering (OSS) design. [http://www.spezialradmesse.de/traix.html]*

The double head tube design is somewhat of a combination between OSS and USS systems: the handlebar is vertical like a traditional upright bicycle's handlebar (with an identical OSS method of motion), but the bottom is connected to a series of linkages that run horizontally to the front wheel, much like the tie rods of the USS design. This model of steering is fairly easy to make and avoids the "tiller" steering of the OSS design, however the linkages are more complicated and require more parts.

To determine our design's optimal steering mechanism, we developed a weighted Pugh chart (Table 2) that took into account cost, comfort, robustness, manufacturability, weight, and ease of brake attachment. We determined that over seat steering was the most suitable system for our vehicle's design.

*Table 2: Steering Design Pugh Chart*.

| **Design Feature** | **Cost** | **Comfort** | **Robustness of steering** | **Manufactur-ability** | **Weight** | **Ease of brake attachment** | **TOTAL** |
|---|---|---|---|---|---|---|---|
| *Weight* | 70 | 20 | 90 | 40 | 50 | 20 | |
| *Multiplier* | .23 | .1 | .3 | .13 | .17 | .07 | |
| Underseat | 1 | 3 | 5 | 1 | 3 | 3 | 2.87 |
| Overseat | 5 | 1 | 1 | 5 | 5 | 1 | 3.13 |
| Double Head Tube | 3 | 1 | 3 | 3 | 1 | 1 | 2.33 |

#### 1.5.3 Drivetrain

The drivetrain system in the human powered vehicle is comprised of all motion and braking functions. More specifically, the drivetrain includes the transfer of power from the rider to the wheels, the transition through gears for maximum efficiency, and the halting of the vehicle. The transfer of power in such a vehicle can be accomplished via a rotary shaft, by a belt driven system, or by a chain driven system. With respect to capability, design simplicity, and overall cost, we determined that the most practical option for our particular vehicle was a chain driven system.

Due to the choice of front wheel steering, the most suitable design for the vehicle would be rear wheel drive. Rotary joints would have to be implemented to supply power to the pivoting front wheels, which would be an inefficient use of space and weight. Additionally, a front wheel drive system would present challenges with traction because the vehicle design has a much higher weight distribution in the rear. Overall, a rear wheel drive system is more practical for our vehicle.

## 1.6 Innovation - Seat Adjustability

In order to compensate for the different height of our riders, our team needed to develop a mechanism that is easily adjustable to allow for easy pit stops when changing riders. We developed a Pugh chart to analyze the importance of each aspect of adjustability and how different designs compare.

*Table 3. Bicycle Adjustability Pugh Chart.*

| **Design Feature** | **Cost** | **Simplicity** | **Adjustment Speed** | **Manufacturability** | **Weight** | **TOTAL** |
|---|---|---|---|---|---|---|
| *Multiplier* | *2* | *2* | *1* | *2* | *1* | |
| Adjustable Seat | + | + | - | + | - | 4 |
| Adjustable BB | 0 | - | + | - | + | -2 |

### 1.6.1 Adjustable Bottom Bracket

Most recumbents on the market today use an adjustable bottom bracket and chain tensioner to account for the different height of riders. An example of this design can be seen in the image below.

*Figure 7: Example of bottom bracket adjustability*

The advantages of this design is that there is a large adjustable range, therefore one can account for large differences in rider height. But with each adjustment, one would also have to adjust the chain length. This can be done manually, by adding individual lengths of chain, or this can be done using a chain tensioner. Both options take considerable time to complete, which is not ideal for a racing competition where one is only allowed limited time in the pit stop. Due to the complexity of the design and requirement of additional tools and bike components, our group decided to pursue other options.

### 1.6.2 Adjustable Seat

Due to the frame design of our bike and the location of the seat, the main beam (boom) offers sufficient distance to account for different rider height. The advantages of using an adjustable seat is that one doesn’t have to adjust the length of the chain with each rider, without worry of an unstable bottom bracket. With an adjustable seat design, the chain will always stay the same length, and the bottom bracket remains secure in one location.

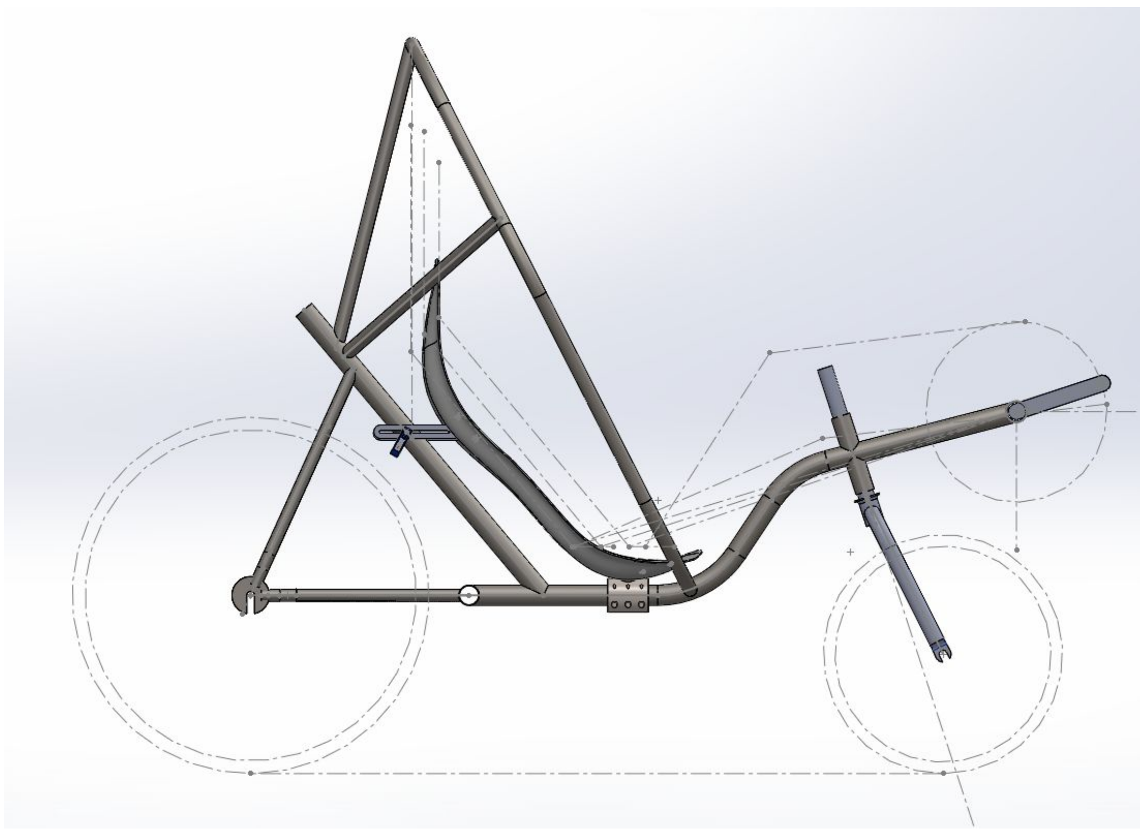

*Figure 9: Side view of bike, showing seat adjustability.*

Our current design consists of two different assemblies: the top seat attachment and the bottom seat attachment. The bottom seat attachment is attached to the boom and supports most of the riders weight. The top seat attachment supports the back of the rider and also reduces the stresses placed on the bottom seat attachment and carbon seat. The bottom seat attachment consists of a tube clamp that moves along the boom and is attached to the carbon seat via a welded tube, plate, and 3D printed former assembly. For the bottom seat attachment, we 3D printed a former to the same curvature as the carbon seat to allow for more support. This will be bolted to a steel plate and the other side of the seat. A short section of mitered tubing is welded to the steel plate and to our tube clamp. For the top seat attachment, we 3D printed another former to the same curvature as the back of the seat and bolted this to a steel plate. We then laser cut steel plating into a slotted bar configuration and used two locking skewers to clamp the slotted bars to the frame and the steel plate tabs that are affixed to the carbon seat.

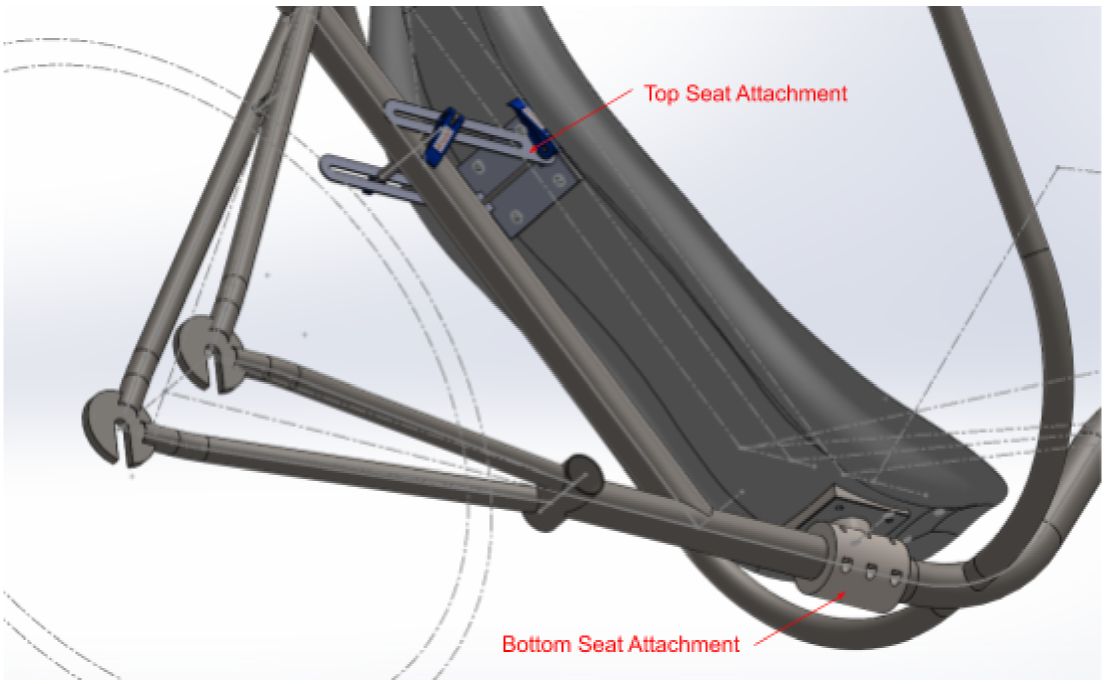


*Figure 10: Both pieces of the Seat Adjustability design*

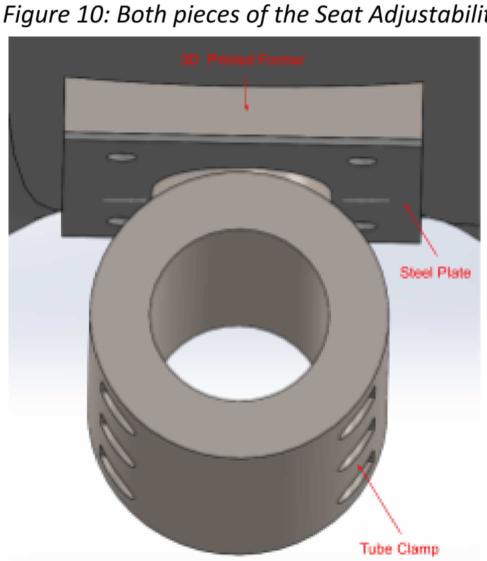


*Figure 11: Bottom Seat Attachment*

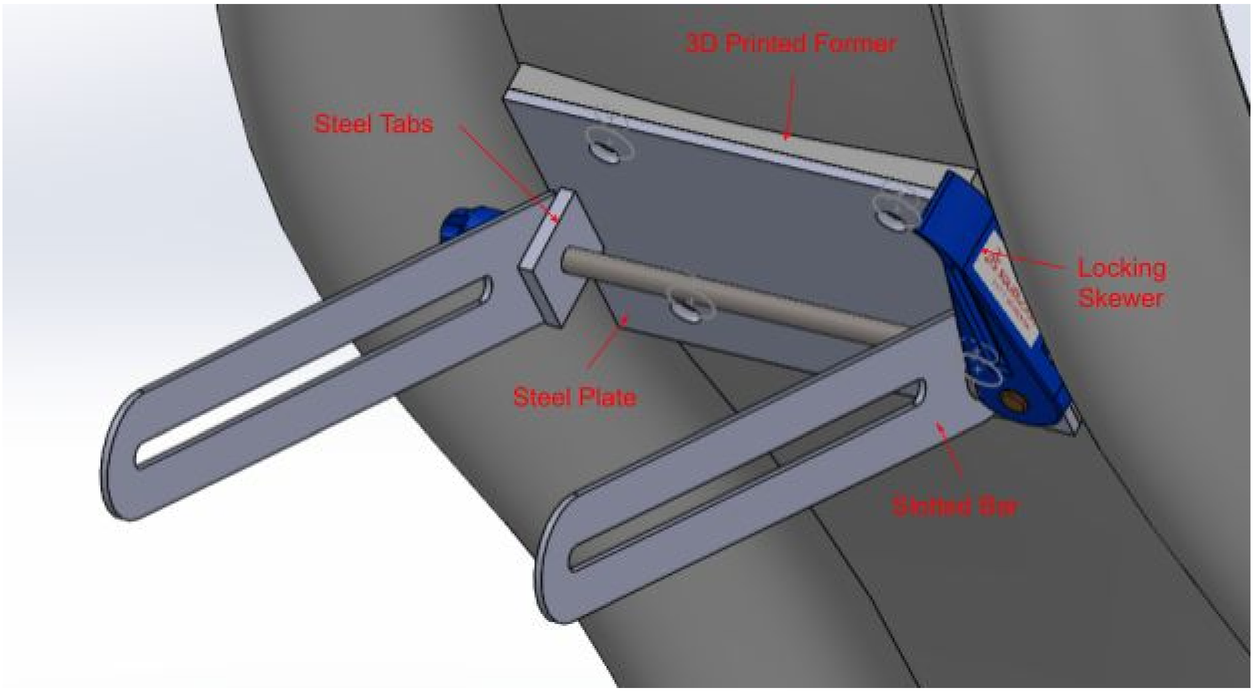


*Figure 12: Top Seat Attachment*

A critical part of our final design was that it does not require high tolerancing for the final machined parts and assembly. Due to our slotted bar configuration and use of the locking skewer, we have plenty of room to adjust for certain errors or tolerances in manufacturing (i.e. seat plane is not parallel to back boom, carbon seat not perfectly symmetrical, etc.).

Our final seat adjustability design allows for 4” of lateral movement along the boom, which allows for ~6” of adjustability for riders. With our design, riders between the height of 5’4” and 5’10” are able to ride comfortable.

## 2. Analysis

### 2.1 RPS Analyses

A model of the bicycle was created using ANSYS Mechanical APDL in order to complete a finite element analysis of our vehicle. Node points were designated and connected using lines and splines, and each segment was identified with its established material properties and geometric dimensions.

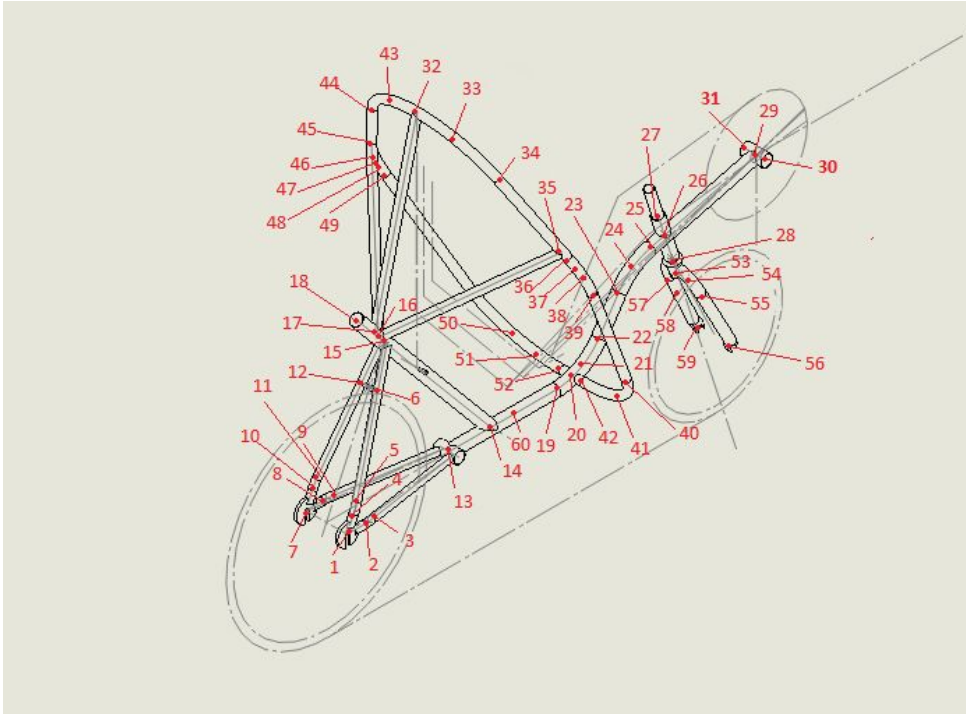

*Figure 13. Choosing the nodes to analyze in APDL*

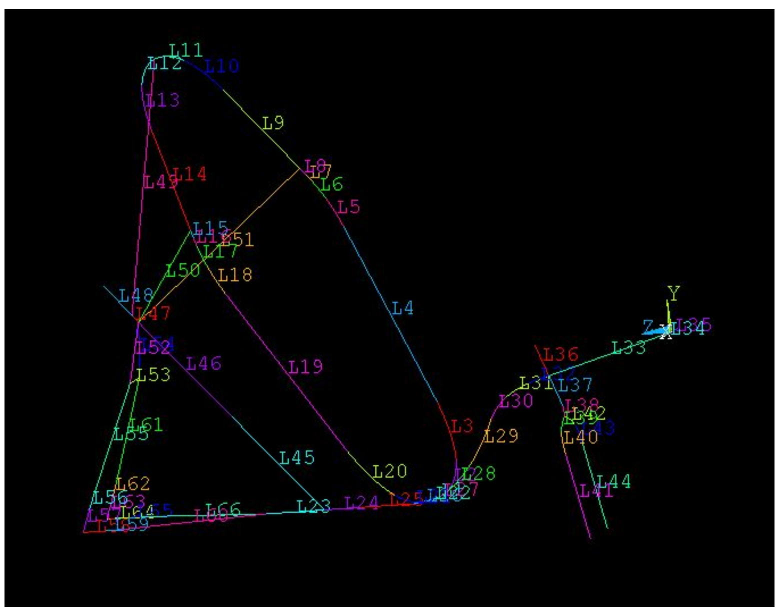

*Figure 14: Converting Nodes into lines and splines with the appropriate geometry on APDL.*

The goal of this analysis was to test the strength and deflection of the roll cage and ensure that our design was safe. The RPS load cases were analyzed to ensure the deflection would not exceed the competition's specifications. The bike was constrained at two harness securement points- one in the middle portion of the back boom support, and the other beneath the rider's seat on the main boom. Thus, in the event of a crash, the harness should safely constrain the rider and prevent injury. First a 2670 N load was applied to the top of the roll cage at an angle of 12° from vertical. We found that the maximum elastic deformation was 5.74 mm which is well below the required 5.1cm. Our goal was to keep the stress below the ultimate stress point (560 MPa) so that even if our bicycle would plastically deform, it would not break under the load. In fact, our bicycle will receive a maximum stress of 295.8 MPa which is less than the yield stress of chromoly steel. This confirms the safety of our vehicle and the rider given the top load.

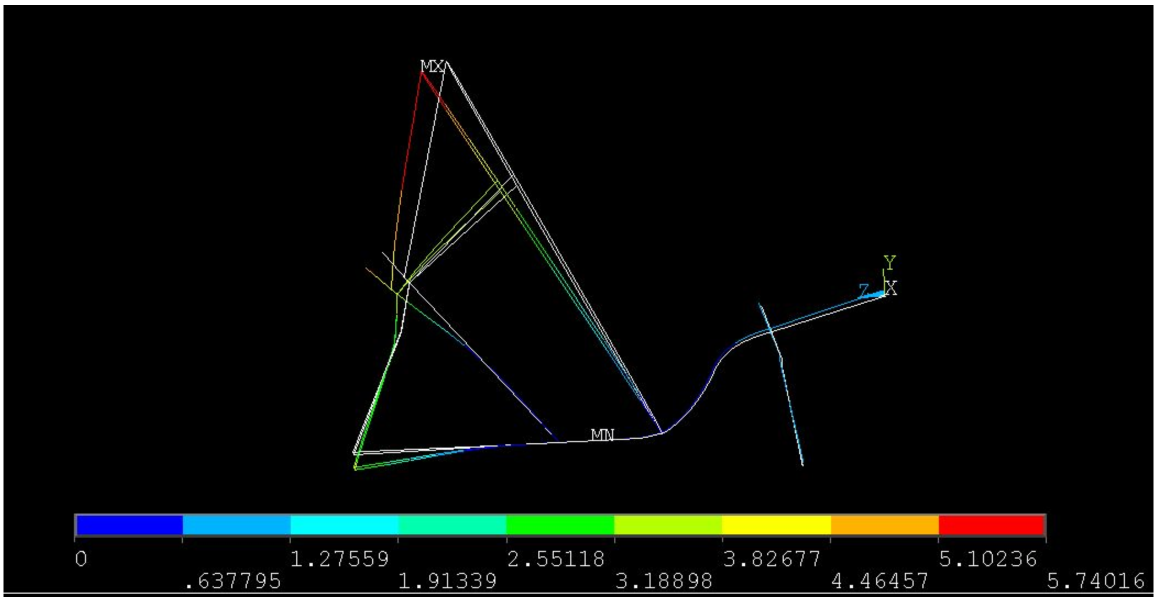


*Figure 15. Deformation of the bicycle with a top load of 2670 N on the roll cage. (units in mm)*

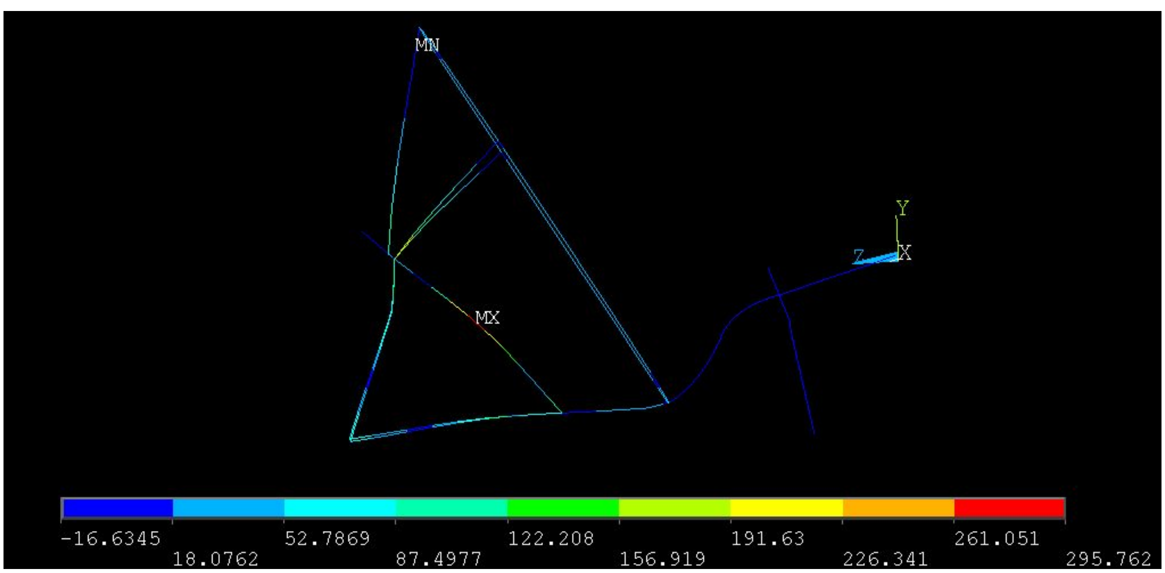


*Figure 16. Combined axial and bending stress of the bicycle with a top load of 2670 N on the roll cage. (units in MPa)*

Next, we performed a similar analysis for a side load of 1330 N on the roll cage. With this, we had to ensure that our deformation was below 3.8 cm. After applying this load to our model, we found that the maximum elastic deformation was found to be 22.34mm, which is within the competition specifications. The maximum stress was discovered to be 346.86 MPa, which again is lower than the yield strength for chromoly. Thus, our design is vetted to be safe for the rider in event of a crash.

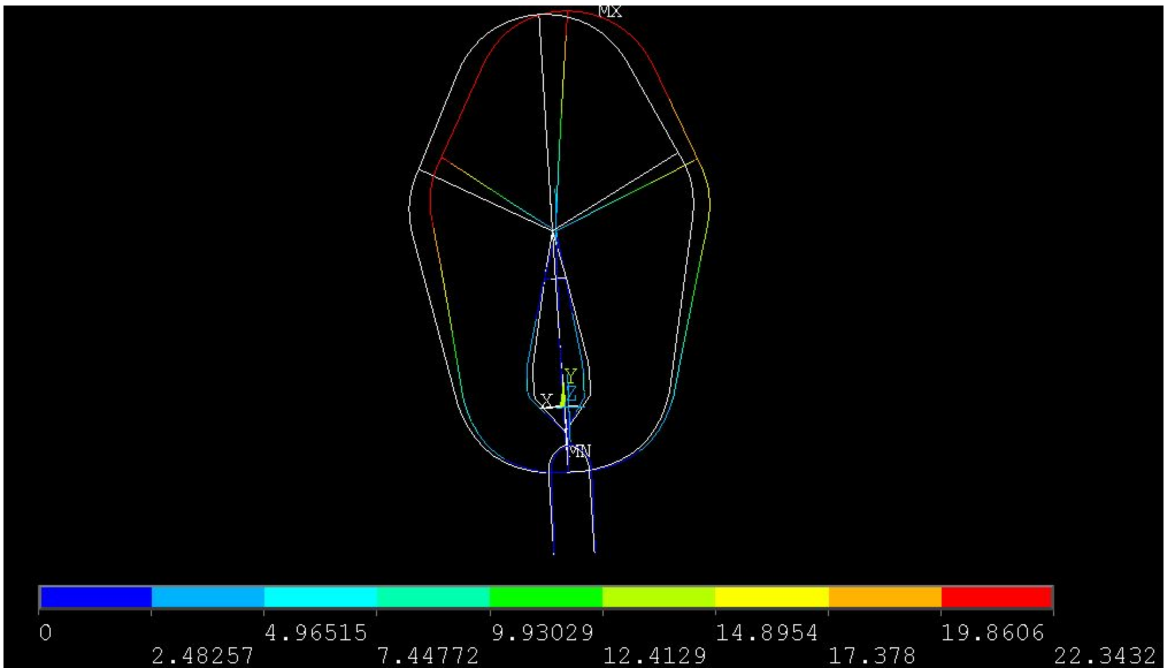


*Figure 17. Deformation of the bicycle with a side load of 1330 N on the roll cage. (units in mm)*

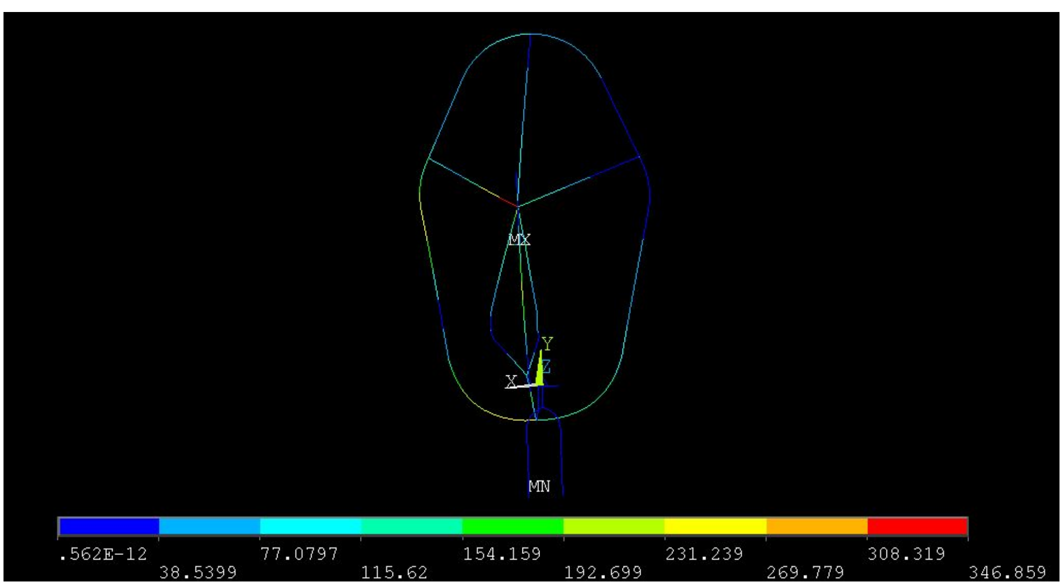


*Figure 18. Combined axial and bending stress of the bicycle with a side load of 1330 N on the roll cage. (units in MPa)*

## 2.2 Structural Analyses

In order to complete a structural analysis for our vehicle, we began with a simplified version of only the main boom. We idealized the bike as a simply supported beam, and only accounted for the weight of a 200lb(889N) rider. The following figure depicts the free body diagram and hand calculations for this method. We wanted to ensure that our main frame design would be able to withstand a rider's load and that the beam would not go above yield stress.

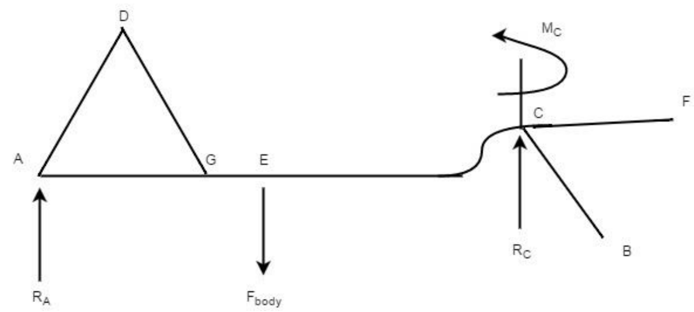


*Figure 19. Free body diagram of main boom with force of static rider.*

In Figure 19, simplistic model of our frame was analyzed with pin supports at Points A and B. The reaction force at B was relocated to C along with a moment-couple in order to calculate this is a simply supported beam. By knowing the distances between the forces, we were able to calculate the reaction forces at A and C as well as the moment at C. Then, by creating shear and moment diagrams, we were able to find the point of maximum stress. The location of the maximum stress was found to be at E, where the rider's center of mass is. The bending stress of the frame using a 1.5" tube with a thickness of 0.065" was found to be 159.9 MPa, by using the equation for bending stress, $\sigma = \frac{Mc}{I}$ where $I = \frac{\pi}{4}(R_o^4 - R_i^4)$ . Using the yield stress of 4130 chromoly, the factor of safety was found to be 2.88 by using the equation for yield factor of safety, $n_y = \frac{S_y}{\sigma}$ .

This model did not include the roll cage and was only meant to be a starting point for the full frame and RPS system structural analysis. We also included an ANSYS model with a static load to represent a person sitting on the bike or riding in a forward direction. An 889N (200lb) person was estimated for this calculation to ensure the heaviest load the bike would endure. The bicycle was constrained at the bottom of the front fork and at the rear dropouts and the force was applied at the rider's approximated center of mass. The maximum deflection with this load was found to be 3.716mm, and the maximum stress was found to be 105.221 MPa which is well below the yield stress of chromoly, which is 460 MPa.

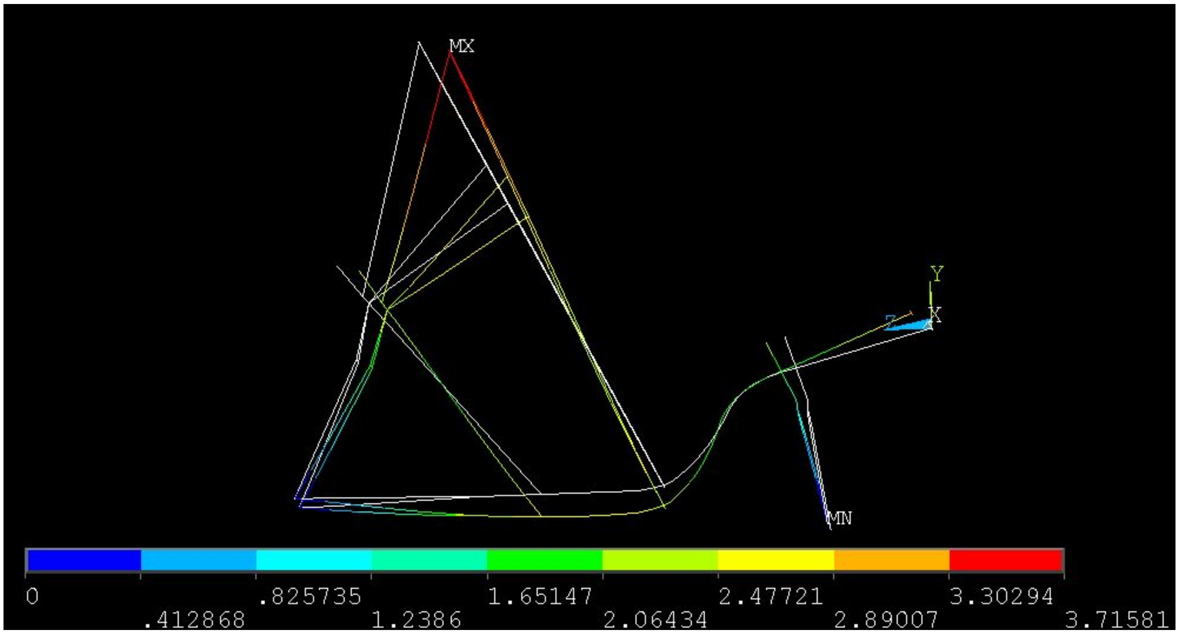


*Figure 20. Deformation of the bicycle with a static 889N load. (units in mm)*

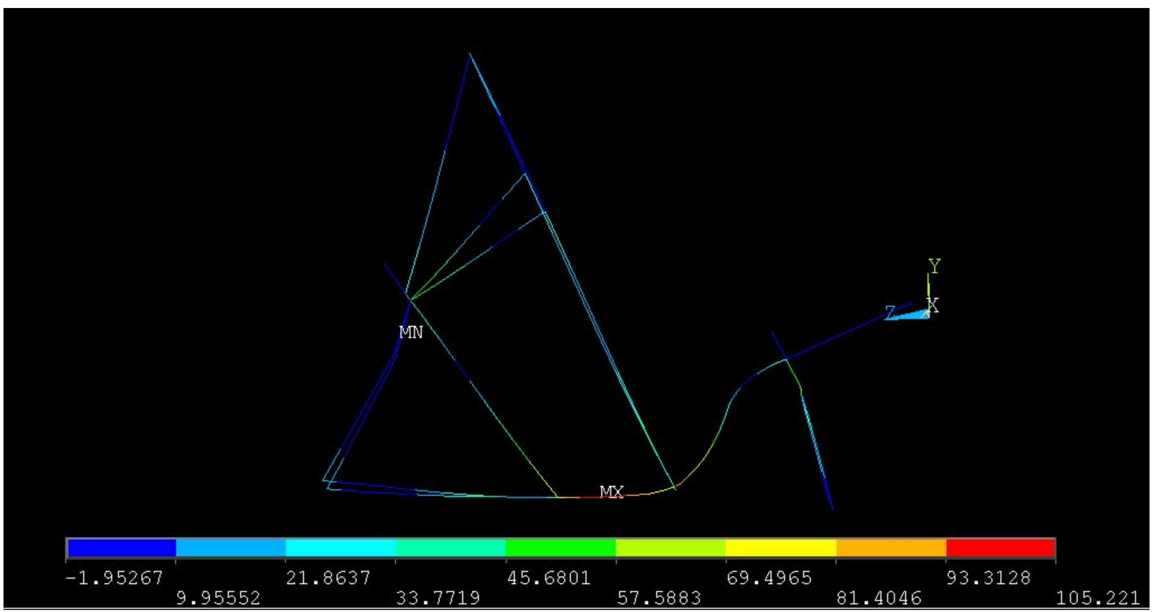


*Figure 21. Combined axial and bending stress of the bicycle with a static 889N load. (units in MPa)*

## 2.3 Aerodynamic Analysis

Due to lack of funds and time, an aerodynamic fairing was not part of this year's vehicle. Consequently, no aerodynamic analysis was completed at this time, but we estimated the coefficient of drag using drag force equations.

## 2.4 Cost Analyses

On paper, the total cost of parts and tooling for Panther 1 came to $1,975.06 as seen in Table 3. Some parts were donated by a local bicycle co-op called the Alley Bicycle Co-op and university professors, helping reduce costs.

*Table 3: Cost Analysis*

| 1 | **Bicycle Specific** | | | | |
|---|---|---|---|---|---|
| 2 | **Part Name** | **Qty** | **Price/part** | **Cost** | **Notes** |
| 3 | Crankset | 1 | $150.00 | $150.00 | |
| 4 | Pedals | 1 | $45.00 | $45.00 | |
| 5 | Chain | 1 | $72.00 | $72.00 | |
| 6 | 9 Speed Cassette | 1 | $106.80 | $106.80 | |
| 7 | Bottom Bracket (68/113) | 1 | $29.00 | $29.00 | |
| 8 | Rear Wheel | 1 | $199.00 | $199.00 | |
| 9 | Derailleurs (rear) | 1 | $64.00 | $64.00 | |
| 10 | Brakes | 2 | $10.00 | $20.00 | |
| 11 | Brake Cables | 2 | $11.00 | $22.00 | |
| 12 | Shifters | 1 | $111.00 | $111.00 | |
| 13 | Recumbent Seat (Carbon) | 1 | $328.00 | $328.00 | Includes shipping |
| 14 | Bottom Seat mount | 1 | $28.00 | $28.00 | |
| 15 | Upper Seat Mount | 1 | $30.00 | $30.00 | |
| 16 | Seat Cushion | 1 | $119.00 | $119.00 | |
| 17 | 20" Front Wheel | 1 | $63.05 | $63.05 | |
| 18 | Sunlite Front Fork | 1 | $60.00 | $60.00 | |
| 19 | 20 in wheel rim strip | 1 | $7.00 | $7.00 | |
| 20 | 20 in tire | 1 | $40.00 | $40.00 | |
| 21 | 20 in tube | 1 | $8.55 | $8.55 | |
| 22 | 1.5" ID Steel Tube Clamp | 1 | $35.99 | $35.99 | 1.5" ID, 3" long?, **1020 steel**, with a clamping force of up to 8,600lbs |
| 23 | M6 Nylon nuts | 1 | $4.00 | $4.00 | for seat |
| 24 | M6 Washers, SS | 1 | $4.00 | $4.00 | for seat |
| 25 | Abrasion-Resistant Cushioning Washer, for 1/4" Screw Size, 0.25" ID, 0.75" OD | 1 | $4.00 | $4.00 | for seat |
| 26 | Harness | 1 | $44.95 | $45 | |
| 27 | LUGLESS BB-SHELL STD 69MM CROMO (69/113) | 1 | $4.25 | $4.25 | English thread, 39.7mm O.D. x 69mm |
| 28 | Head Tube OS CRMO 36.0SM x 200 | 1 | $7.87 | $7.87 | OS HEADTUBE FOR 28.6 FORK STEERER, FITS STANDARD HEADSETS, 36.0 x 1.1 x 200mm, 33.8mm I.D. |
| 29 | NOVA CRMO 22mm ROUND CHAINSTAY | 1 | $15.94 | $15.94 | 22.2 x 0.8 x 440mm long x 12.5 on small end. 1.3 wall on small end. 290mm long taper. |
| 30 | NOVA CRMO ROAD 14mm SEATSTAYS SINGLE TAPER | 1 | $17.27 | $17.27 | 14mm x 0.7mm x 560 long x 10.5 on small end, a 0.9 wall on the small end, 290mm long single taper |
| 31 | DROPOUT REAR VERTICAL 65 DEGREE ANGLE 2-EYELET | 1 | $9.40 | $9.40 | |
| 32 | 506B BRAKE BRIDGE 75mm long | 1 | $5.75 | $5.75 | Length of taper = 30mm. large diameter of tapered part = 12.2mm. small diameter of tapered part = 10.8mm. total length = 75mm |
| 33 | CABLE STOP SINGLE FLAT FRONT KI8 | 10 | $0.27 | $2.70 | 4 for rear brake, 4 for rear shifter |
| 34 | HYDRO BRAKE CABLE GUIDE/ ZIP | 10 | $0.99 | $9.90 | Cable guides to be used with zipties |
| 35 | M6x25 bolts SS | 1 | $7.22 | $7.22 | for seat, pack of 25 |
| 36 | Low-Carbon Steel Tubing, 1.5" OD, 1.370" ID, .065" Wall Thickness | 1 ft length, quantity 1 | $4.53 | $4.53 | Test piece for bending |
| 37 | Easy-to-Weld 4130 Alloy Steel Round Tube, 1.500" OD, .058" Wall Thickness | 1 ft length, quantity 1 | $11.67 | $11.67 | Test piece for bending |

| | | | | | |
|---|---|---|---|---|---|
| 38 | Easy-to-Weld 4130 Alloy Steel Round Tube, 1.000" OD, .058" Wall Thickness | 1 ft length, quantity 1 | $9.41 | $9.41 | Test piece for bending |
| 39 | Easy-to-Weld 4130 Alloy Steel Round Tube, .875" OD, .049" Wall Thickness | 9ft legnths, quantity 3 | $28.74 | $86.22 | 22.2mm OD, 1.2446 mm thickness |
| 40 | | | **Total** | $1,787.47 | |
| 41 | | | | | |
| 42 | **Jig Specific** | | | | |
| 43 | **Part Name** | **Quantity** | **Price/part** | **Cost** | **Notes** |
| 44 | 8020 T-slot Framing | 30 ft. | $31.59 per 10 ft | $94.77 | |
| 45 | T-slot extended plates | 6 | $6.74 | $40.44 | |
| 46 | T-slot 90 degree plates | 4 | $8.47 | $33.88 | |
| 47 | T-slot fasteners | 10 | $1.85 | $18.50 | |
| 48 | | | **Total** | $187.59 | |
| 49 | | | | | |
| 50 | | | **GRAND TOTAL** | $1,975.06 | |

## 2.5 Product Lifecycle Energy/CO2 Analysis

To assess the product life cycle of the vehicle we analyzed the energy invested in production and $CO_2$ generated during all stages of the product's life, from raw material extraction to end of life recycling.

### Lifecycle Parameters

The production of the vehicle was broken down into discrete processes. Each process was evaluated by assessing the energy (J) required for the process and the amount of $CO_2$ it generated.

Energy required for raw material extraction were calculated based on a large model iron mine using the *SHERPA Mine Cost Estimating Model*.

Required energies for steel production were based on theoretical minimum energy scenarios. While minimum energy scenarios are not representative of real-world processes, these values offer an absolute minimum which may be scaled to represent selected real-world manufacturing process. The various components of the vehicle make use of different steel production processes, so to account for this variation we imagine a best case scenario where all steel is produced using minimum energy investment. This case assumes ore is pure $Fe_2O_3$, no superheating, and the product is cast into its final shape without finishing.

End life energy and emissions was determined by quantifying the energy usage required to recycle the metal components of the vehicle back into steel mill product.

*Table 4: Product Lifecycle Energy/$CO_2$*

| Raw Material Extraction | | | |
|---|---|---|---|
| **Process** | **MJ/tonne of Ore** | **kgCO2** | **Ref.** |
| Drilling | 1.99 | | [US D.O.I.] |
| Blasting | 3.37 | | |
| Loading | 7.34 | | |
| Haulage | 59.15 | | |
| Miscellaneous | 7.54 | | |
| **Total** | 79.39 | 3,088,141 | |

| Material Refining | | | |
|---|---|---|---|
| **Process** | **MJ/tonne** | **kgCO2** | **Ref.** |
| Theoretical Minimum Energy | 8620 | 4,632,212 | [DOE] |

| Manufacturing & Assembly | | |
|---|---|---|
| **MJ/day** | **kgCO2** | **Ref.** |
| 125.5 | 108 | [Inside Energy] |

| Recycle Production and Processing | | |
|---|---|---|
| **MJ/tonne** | **kgCO2** | **Ref.** |
| 1600 | 19.02 | [DOE] |

## Lifecycle Analysis

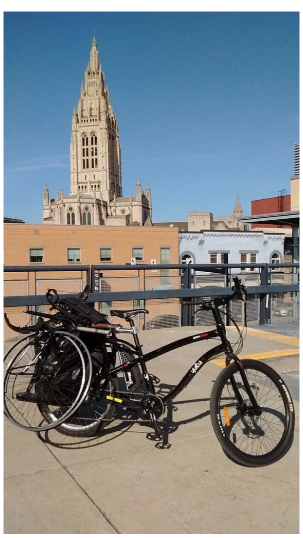

When possible, the team sourced stock parts from local retailers. Pickups were performed using cargo bikes to foster a holistic commitment human powered transportation amongst the team. Confusing production chains made it difficult to do detailed analysis of each component of the vehicle, so we evaluated the vehicle as a whole based on the masses of materials which comprise it. On a yearly basis, 625 MJ must be expended to produce and operate our vehicle and 7,456 Mg of $CO_2$ would be generated. Compared to a typical mid-sized sedan, our vehicle production consumed 98.7% less energy and produced 98.5% less $CO_2$.

# 3. Testing

The construction of the vehicle has not been completed. Therefore, results and conclusions of the RPS, developmental and performance tests will be presented with the design presentation.

## 3.1 RPS Testing

The objective of the RPS test is to ensure the safety of the rider in the event of an accident as well as be within the rules of the competition. The top load will be tested with a static weight equal to or exceeding 2670 N with the RPS secured at a 12° from the vertical axis with the vehicle secured in place to create a resultant force at the roll bar attachment. The side load will be tested by securing the vehicle in place and applying a 1330 N force to the roll bar at the rider's shoulder height.

### 3.1.1 Ergonomics Test

Our SolidWorks model incorporates measurements to account for shoulder width, hip width, and torso height of the largest rider. To test these dimensions in physical space, we used a 1" diameter piece of conduit and 1-to-1 printout of the roll cage and frame to make a rough "pretotype" of our design. From this pretotype we concluded that the shoulder width could be reduced by 5 cm on either side.

*Figure 22: Testing the ergonomics of our conduit frame and roll cage.*

## 3.2 Developmental Testing

### 3.2.1 Tube Bending Test

The HPV has two tubes that require bending, which can be accomplished with the Swanson Center of Product Innovation (SCPI) tube bender. However we first needed to test the bender to see its strength and ability as well as confirm that it will physically be able to bend the tube size and thickness specified in our design.

*Figure 23: Using a manual tube bender to practice bending a roll cage out of conduit.*

The three club members attempted to bend a 1” tube of 4130 chromoly steel with a thickness of 0.065,” a tube size that we specified in the roll cage. The process was difficult to bend to such a small radius, so the bends on the roll cage were adjusted to be greater than 8”.

### 3.2.2 Laser Cutter Mitering Test

The design of the vehicle requires miter cuts at the joints of the tubing. Our school’s machine shop recently obtained a laser cutter with a fourth axis, making it possibly to cut cylindrical surfaces. A mitering test was conducted on a scrap piece of 1”x 0.065” 4130 chromoly tubing and the test was successful. The caveat is that the laser cutter can only miter straight lengths of tube.

*Figure 24: Mitered tube of 4130 chromoly using the laser cutter.*

### 3.3 Performance Testing

The following pre-competition testing will be completed once the vehicle is built:

- Steering test - complete a turn within an 8 meter radius
- Braking test - stop from a speed of 25 km/hr in a distance of 6.0 meters
- Stability test - remain upright for at least 30 meters while traveling at 5-8 km/hr
- Adjustability test - check compatibility with riders of different heights. When the seat is adjusted properly, riders from 5'4" to 6'0" should have a 10° bend in their knee when the pedal is at the furthest point from the rider. This metric will ensure maximum power output.

## 4. Safety

### 4.1 Design for Safety

#### 4.1.1 Harness Attachment Points

In order to ensure rider safety we must make sure that the harness and the bolting points will not fail.

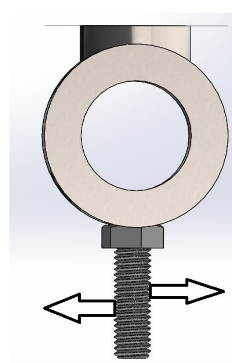

*Figure 25: Location of the harness attachment points below the seat.*

A threaded rod or screw will be attached to the bottom clamp as shown above. The steel plates of the harness will then slip over the rod and be bolted in place. This will cause the rod to be in single shear when the weight of the rider is transferred to the harness. For a 1/2" threaded steel rod, the allowable shear stress is 72 ksi and the effective sheared area of the rod is 0.196 $in^2$. Using this information we can solve for the maximum the bolting point can withstand. Letting $\tau_{max} = \frac{P}{A}$ we can solve for P and with a factor of safety of 4 we obtain a maximum allowable load of 3,500 lbs. Even if a 200 lb rider flipped the vehicle and their entire weight hung from the bolt, the allowable shear stress would not be exceeded and the rod would not fail in shear.

## 4.2 Hazard Analyses

The main safety features of the vehicle are well-integrated into the design of the vehicle and do not hinder proper use of the vehicle. In particular, the roll cage plays a key role in the structural integrity of the vehicle's frame, which means that in the event of a crash, the roll cage can support the weight of the rider and deal with additional forces associated with the crash. In combination with a safety-rated harness, the roll cage will keep the rider safe during normal collisions and accidents. In minor accidents, the rider can easily put their feet down to regain balance, thanks to the low-to-the-ground rider position.

Rider fit is a very important but often overlooked part of the overall safety of a vehicle's design. If a rider does not fit properly in the vehicle (correct leg extension, comfortable reach, access to controls, etc.), they cannot operate it safely as it was designed to be operated. To deal with this, we designed our vehicle to be adjustable for many different rider sizes.

The rider-to-vehicle relationship was also optimized for safety and ergonomics. Any location where the rider could come in contact with the vehicle is to be sanded smooth to eliminate sharp edges where a rider's clothing can get caught. The roll cage was designed to protect the rider's head and arms, and we plan on incorporating a hoop enclosure in the front of the vehicle to protect the rider's legs from injury.

Another important aspect of safety that must be considered is that of those around the vehicle. To help aid in visibility and reduce the chances of accidents, head and tail lights, a bell, and reflectors are included in the vehicle's design. These will reduce the chance of a pedestrian or other rider not seeing our vehicle and stepping out in front of it at an intersection. As a final measure of safety, highly reflective paint or tape will also be used to accent the upper portions of the roll cage. This will increase the vehicle's visibility in low-light situations. In particular, this addition will decrease the chance of collision by an automobile, especially at night.

Precaution was taken during the building and fabrication of the vehicle. All welding, brazing, cutting, and assembling was conducted in university spaces that are outfitted with safe equipment. In order to use these spaces, all team members had to go through in-depth safety training for all of the machines before they could use them. Anyone working on the vehicle also was required to wear proper personal protective equipment.

# 5. Conclusion

## 5.1 Comparison – Design goals, analysis, and testing

Load requirements, as specified by ASME 2017 Rulebook, for the rollover protection system were met according to an ANSYS APDL analysis. With the specified top load, the roll cage deflects only 0.574 cm which is well under the allowable 5.1 cm. The side load deflects the roll cage 2.234 cm which is well under the allowable 3.8 cm.

*Table 5: Load Specification Requirements for Rollover Protection System*

| | Top Load | Side Load |
|---|---|---|
| Allowable Elastic Deformation | 5.1 cm | 3.8 cm |
| Elastic Deformation as Revealed by Analysis | 0.574 cm | 2.234 cm |

## 5.2 Evaluation

The vehicle met all goals set forth by the team. Budget constraints were achieved through careful planning and organization, with necessary compromises made in a way that would not affect the overall quality of the vehicle. To ensure functionality, the vehicle will be extensively tested upon completion of assembly to ensure all riders are confident when riding the vehicle, and that all systems perform as expected. Adjustability for various sized riders was achieved by utilizing an adjustable seat. As a result of this integrated design, the vehicle can accommodate riders whose height ranges between 5’4” and 6’. Final weight will be determined upon completion of the vehicle; however, initial estimates put the vehicle weight at approximately 40 lbs. Finally, the structural design and rollover protection design was evaluated using hand calculations and finite element analysis (FEA) to ensure the required loading constraints were met. Additional testing will be performed upon completion to validate FEA results.

Furthermore, the vehicle was designed with manufacturability in mind. Tube bending, mitering, and welding processes available to the team aided in determining the final design. Chromoly 4130 steel was chosen to be a suitable material to construct the frame and rollover protection system with due to its weldability and ability to be mitered using a laser cutter. Tube bending capabilities determined what bend radii and tube size options were possible.

However, the final design still was chosen with ergonomics, performance, and safety in mind. With that, the design process proved to be a balance between manufacturability and functionality in mind. An ANSYS analysis showed that the roll cage would elastically deflect less than 5.1 cm when applied with the top load of 2670 N at an angle of 12 from the vertical. Another analysis revealed that our roll bar would elastically deform less than 3.8 cm when applied with a 1330 N load from the horizontal at shoulder height.

## 5.3 Recommendations

In the future, the design will be improved. The ANSYS ADPL analysis will aid in future improvements to be made in optimizing the frame and roll over protection system in terms of strength, stiffness, and weight. More focus could be put into designing a fairing system and performing an aerodynamic analysis. We recommend manufacturing before March of the competition year.

## 6. References

[1] Surly Bikes, 2017, "Long Haul Trucker Geometry,"
http://surlybikes.com/bikes/long_haul_trucker/geometry
[2] Dunford, Aaron, Dec. 11 2017, "Bikefit Series - Breaking Down Bike Geometry,"
http://www.bicycles.net.au/2015/12/bikefit-series-breaking-down-bike-geometry/
[3] Recumbent-cycle.com, Aug. 4 2012, "Optima Lynxx,"
http://www.recumbent-cycle.com/en/recumbent-bike/55-optima-lynxx
[4] Brown, Sheldon, 2007, "Tire Sizing Systems,"
http://www.sheldonbrown.com/tire-sizing.html
[5] Budynas, Nisbett, 2014, "Theoretical Stress Concentrations,"
https://disbasicoupiita.files.wordpress.com/2013/03/factor-concentracion-esfuerzos.pdf
[6] Pilkey, W. D., & Pilkey, D. F. (2008). *Peterson's Stress Concentration Factors, 3rd Edition*. John Wiley & Sons.
[7] 2017, "Factor of Safety FOS Review"
http://www.engineersedge.com/analysis/factor-of-safety-review.htm
[8] Freuhan, R.J., Fortini, O., Paxton, H.W., and Brindle, R., 2000, "Theoretical Minimum Energies to Produce Steel for Selected Conditions,"
http://energy.gov/sites/prod/files/2013/11/f4/theoretical_minimum_energies.pdf
[9] DOE, "Energy and Environmental Profile of the U.S. Mining Industry"
https://energy.gov/sites/prod/files/2013/11/f4/iron.pdf